



Characterizing the rainy season of Peninsular Florida

Vasubandhu Misra^{1,2,3} · Amit Bhardwaj^{1,3} · Akhilesh Mishra^{1,4}

Received: 23 June 2017 / Accepted: 6 November 2017 / Published online: 18 November 2017
© Springer-Verlag GmbH Germany, part of Springer Nature 2017

Abstract

Peninsular Florida (PF) has a very distinct wet season that can be objectively defined with onset and demise dates based on daily rainfall. The dramatic onset of rains and its retreat coincides with the seasonal cycle of the regional scale atmospheric and upper ocean circulations and upper ocean heat content of the immediate surrounding ocean. The gradual warming of the Intra-Americas Seas (IAS; includes Gulf of Mexico, Caribbean Sea and parts of northwestern subtropical Atlantic Ocean) with the seasonal evolution of the Loop Current and increased atmospheric heat flux in to the ocean eventually enhance the moisture flux into terrestrial PF around the time of the onset of the Rainy Season of PF (RSPF). Similarly, the RSPF retreats with the cooling of the IAS that coincides with the weakening of the Loop Current and reduction of the upper ocean heat content of the IAS. It is also shown that anomalous onset and demise dates of the RSPF have implications on its seasonal rainfall anomalies.

1 Introduction

The Peninsular Florida (PF) region with its unique geography in the continental United States, surrounded by relatively warm oceans in the boreal summer and fall seasons has a very distinct wet season (Misra and DiNapoli 2013). The relative abundance of fresh water resource in Florida primarily stems from this seasonality of the rainy season of PF (RSPF) that recharges the groundwater in one of the largest aquifers of the world, the Floridian aquifer and as well as replenishing the fresh water lakes and streams downstream (Davis 1996; Price and Swart 2006). The unique ecosystems of the Everglades and hundreds of miles of Mangroves owe their existence to this unique climate of the PF (Brezonik

et al. 1983; Webb 1990; Obeysekera et al. 1999). The demand for fresh water is rapidly increasing with the growing population and increased diversification of the state's economy from various forms of tourism to water demanding agriculture and mining (Webb 1990). In fact, Carr and Zwick (2016) report that the water demand of cities and suburbs in Florida could double by 2070 from the current values owing to population growth alone. In such a scenario, it is rather important to understand the seasonality of the RSPF, especially when future global climate change impacts on the regional climate of Florida is assessed and interpreted. It is with this intent that we have analyzed the RSPF from available observations, atmospheric and oceanic reanalysis.

A significant number of earlier studies have been devoted to understand the winter season rainfall variations of Florida (Ropelewski and Halpert 1987; Schmidt et al. 2001; Nag et al. 2015). This is largely because of the robust teleconnection displayed by El Niño and the Southern Oscillation (ENSO) on the winter rains of Florida that has led to useful seasonal regional predictability of the hydroclimate (Stefanova et al. 2012). In comparison there are fewer studies examining the RSPF (Misra and DiNapoli 2013). The lack of predictability of the summer seasonal rains over PF as noted in Stefanova et al. (2012) could be partly a reason for this. But variations of the North Atlantic Subtropical High (NASH; Li et al. 2011) and the size of the Atlantic Warm Pool (AWP; Misra and DiNapoli 2013) have been identified as some of the primary drivers of the interannual variations

Electronic supplementary material The online version of this article (<https://doi.org/10.1007/s00382-017-4005-2>) contains supplementary material, which is available to authorized users.

✉ Vasubandhu Misra
vmisra@fsu.edu

- ¹ Center for Ocean-Atmospheric Prediction Studies, Florida State University, Tallahassee, FL, USA
- ² Department of Earth, Ocean and Atmospheric Science, Florida State University, Tallahassee, FL, USA
- ³ Florida Climate Institute, Florida State University, Tallahassee, FL, USA
- ⁴ Center for Ocean-Atmospheric Science and Technology, Amity University Rajasthan, Jaipur, India

of the RSPF. Nonetheless, understanding the seasonality and the variations of RSPF is important, especially when a significant fraction of the annual rainfall is accounted by it.

2 Datasets and methodology

We have used $0.5^\circ \times 0.5^\circ$ gridded rainfall analysis over the US from the National Centers for Environmental Prediction (NCEP) Climate Prediction Center (CPC) (Xie et al. 2007; Chen et al. 2008). This rain gauge based analysis covers the Continental US and is available at daily interval from 1948 to 2005. We have also used the Coupled Forecast System Reanalysis (CFSR; Saha et al. 2010) for analyzing the upper air and upper ocean variables to discern their seasonal evolution with the daily rainfall over the PF. The analysis with CFSR covered the time period of 1979–2005. The use of this reanalysis is not critical to establish the features described in the paper. However, the coupled ocean–atmosphere feature of this reanalysis makes accessibility of upper air and oceanic variables convenient and consistent to conduct analysis outlined in the paper. Further, the features described in the paper are so robust that any analysis of comparable fidelity should display them as well.

The objective definition of onset and demise of the RSPF follows from Noska and Misra (2016). In that study, the Indian summer monsoon was the target, which has a well-known seasonality. In a similar manner, we define the onset and demise based on the inflection points of the cumulative daily anomaly of rainfall given by:

$$P'_n(k) = \sum_{m=1}^k \left[P_n(m) - \bar{P} \right] \quad (1)$$

where, $P_n(m)$ is the area average daily rainfall for day m of year n averaged over terrestrial PF, \bar{P} is the corresponding annual mean climatology of the rainfall. It is important to note that Eq. (1) is based on area averaged rainfall over PF. In order to relate the seasonal cycle of rainfall to large-scale changes in the atmosphere and ocean, rainfall would have to be area averaged to be consistent with the spatial scales in consideration (Noska and Misra 2016). Moreover, Misra and DiNapoli (2013) show that the rainy season can be distinctly identified across PF (from the southern tip of Florida to the northern limit extending up to Jacksonville). The minimum (maximum) in $P'_n(k)$ is defined as onset (demise) date of the RSPF (Fig. 1). However, there is a minority of years (e.g. 1958, 1977, 1987, 1997) where the seasonal cycle of RSPF is not very well defined (Fig. S1). In such cases to avoid unrealistic diagnosis of the wet season length we add additional conditional statements to identify onset and demise dates. This is enabled by searching for inflection points in

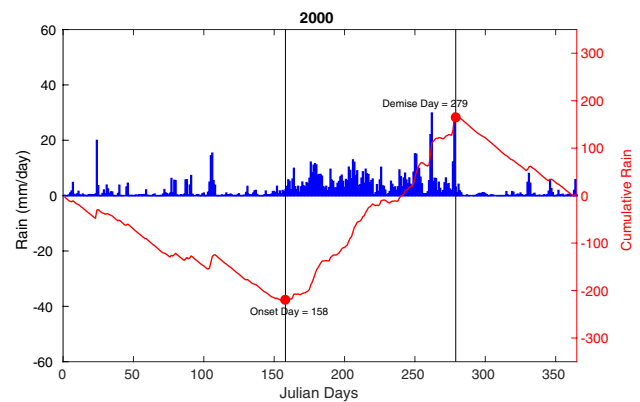


Fig. 1 A schematic illustration of the time series of daily rainfall (blue bars; mm day^{-1}) and its corresponding cumulative daily anomaly (P' in Eq. 1; red line; mm) averaged over PF for the year 2000. The onset (26 May) and demise (28 September) dates of the RSPF are indicated

the daily cumulative anomaly curve of rainfall ($P'_n(k)$) after (before) the first (last) 90 (60) days of the year for determining the onset (demise dates) of the RSPF given that climatological onset and demise dates are 142 (21 May) and 283 (10 October) Julian day respectively. It may also be noted that the time series of the onset and demise dates and therefore the length of the RSPF season has statistically insignificant linear trends (Fig. S2).

3 Results

3.1 Seasonal evolution of the rainy season of Peninsular Florida

A composite of daily rainfall 30 days prior and after the onset date of the RSPF is shown in Fig. 2. It is apparent from this composite that there is a dramatic increase in the daily rain rates ($\sim 9 \text{ mm day}^{-1}$) on the day of the onset (day 0) relative to the day prior to it ($\sim 3 \text{ mm day}^{-1}$). Further, this higher rain rate is sustained after the onset date, which marks a distinct difference on days prior to the onset date of the RSPF. We further illustrate this feature by showing an example of this evolution of rainfall around the date of the onset for the year 2000 (Fig. S3). We clearly observe that in the instance of year 2000 there is a significant break out of rainfall across central and southeastern Florida on the day of onset (June 8) that gives rise to dramatic increase in the area average rainfall over PF (Fig. S3).

Similarly, the daily rainfall of the RSPF retreats as dramatically at the time of the demise date (Fig. 3). The rain rate drops from day -1 (prior to demise date) to day 0 of the demise date from $\sim 9 \text{ mm day}^{-1}$ to around 3 mm day^{-1} . This is yet again illustrated for the year 2000 in Fig. S4, where

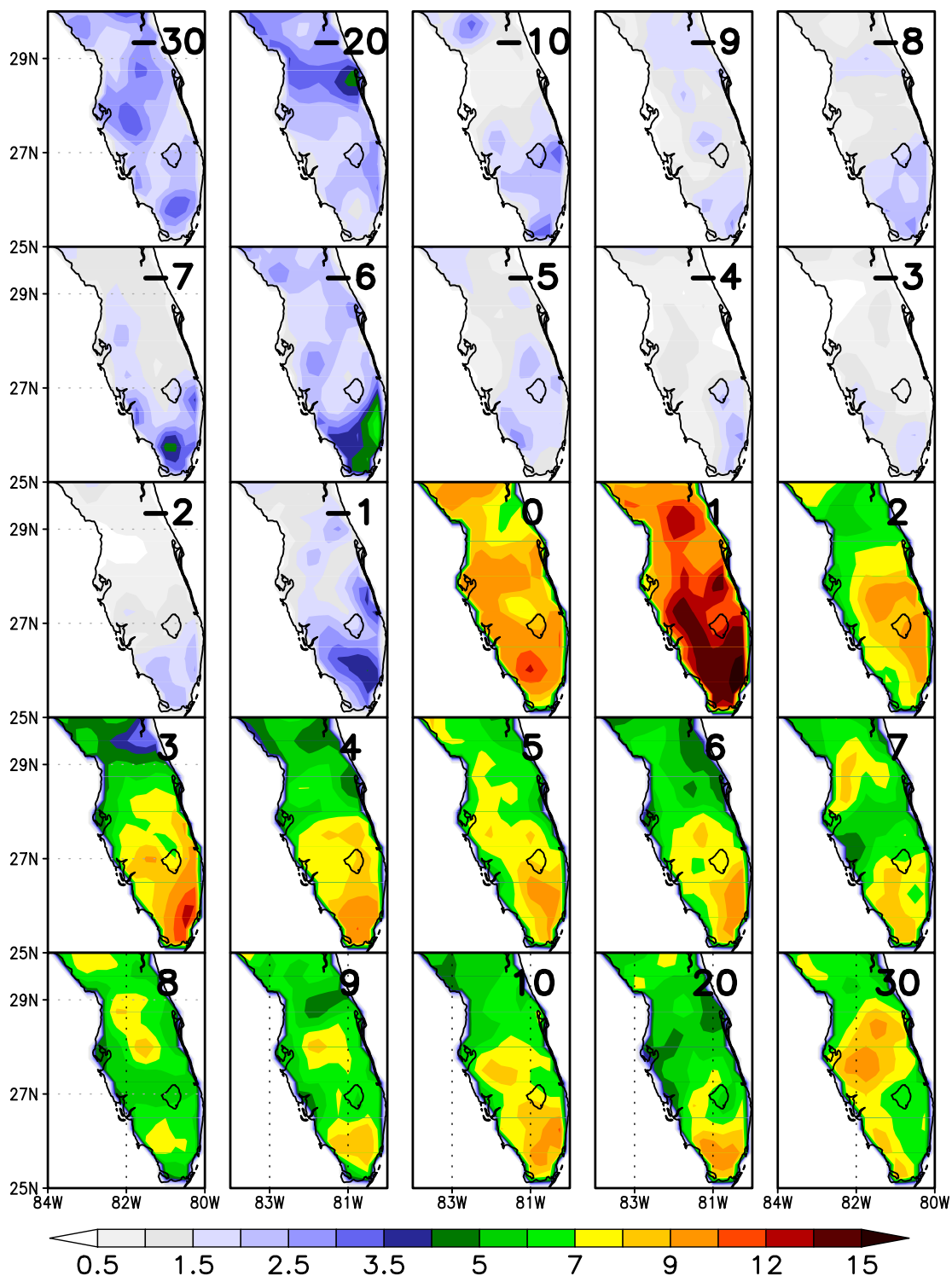


Fig. 2 Seasonal evolution of the daily composite of rainfall (averaged over 58 years from 1948 to 2005) of the RSPF prior to, at, and after the onset date. The days prior and post onset date (day 0) is indicated in the top right corner of each panel. Units are in mm day^{-1}

the rain rate in southwestern and across southeastern-central Florida is in excess of 40 mm day^{-1} on day -1 , which drops

to half as much by day 0 (the day of the demise) and diminishes further by day + 1, after the demise date.

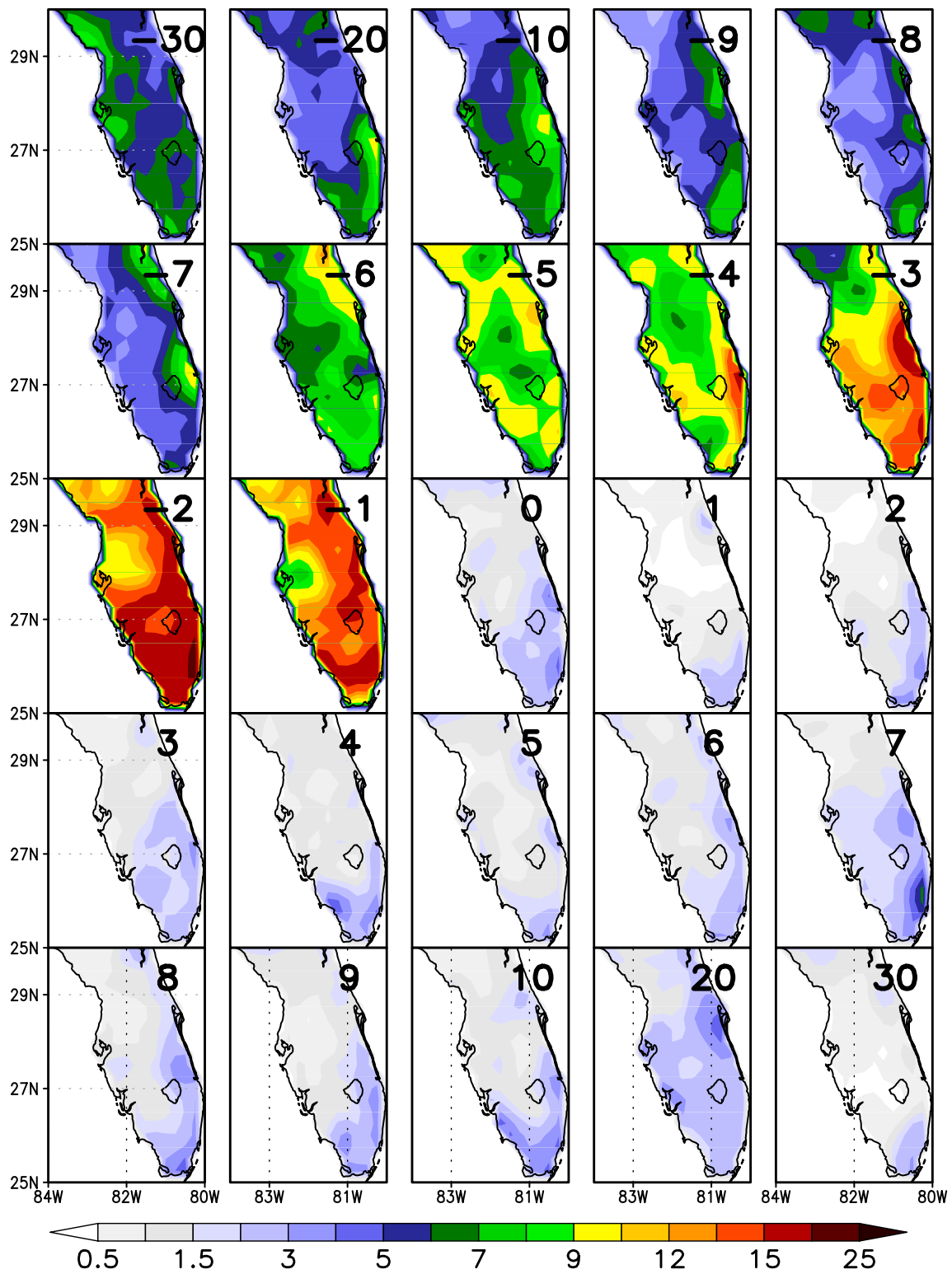


Fig. 3 Seasonal evolution of the daily composite of rainfall (averaged over 58 years from 1948 to 2005) of RSPF prior to, at, and after the demise date. The days prior and post onset date (day 0) is indicated in the top right corner of each panel. Units are in mm day^{-1}

3.2 Seasonal evolution of the wind and mass field

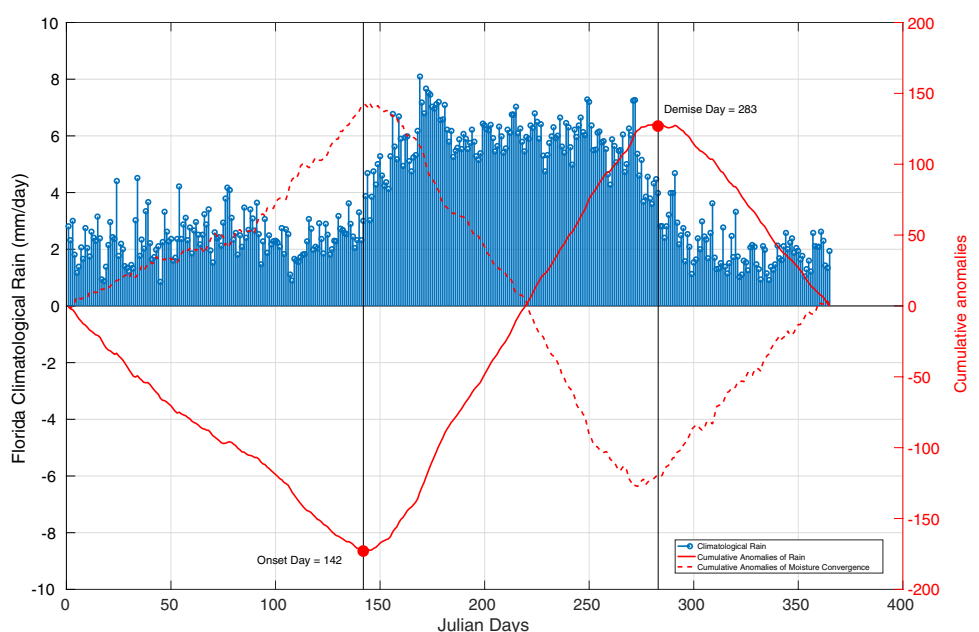
The composite seasonal evolution of the wind field and temperature at 850 hPa centered around the onset of the RSPF is shown in Fig. S5. The higher latitude westerlies continue to extend over PF at 30 days prior to the onset date (Fig. S5). At the time of the onset of the RSPF (day 0, which is ~21 May), there is a low-level trough over the Atlantic with a trailing cold front observed by the accompanying thermal gradients (oriented nearly in the north–south direction over PF) with northerlies and northwesterlies dominating the flow over PF. This would suggest that the uplift provided by the last vestiges of the mid-latitude synoptic frontal systems are triggering the onset of the RSPF. Further, the tropical easterlies are confined to latitudes south of 20°N at and before the day of the onset of the RSPF. However, in the subsequent days, the tropical easterlies expand meridionally and begin to recurve into southerlies and southeasterlies west of around 70°W as part of the western edge of the NASH (Fig. S5).

Similarly, the composite 850 hPa circulation around the time of the demise of the RSPF continue to be dominated by the tropical easterlies and its associated southeasterly flow from the Intra-Americas Seas (IAS; includes Gulf of Mexico, Caribbean Sea and parts of northwestern subtropical Atlantic Ocean) in to Peninsular Florida (Fig. S6). This flow pattern continues for a few days (through day 9) after the demise date (day 0) before the easterlies recede further south in the region (in days 20 and 30 after the demise date; Fig. S6). It is notable that cyclonic features that resemble tropical cyclones appear in the vicinity of PF prior to the demise date in Figure S6. We observe that in the 58 years (1948–2005) of the dataset used in the study for the analysis, there were

26 years that had landfalling tropical cyclones over Florida in early to mid-October (the month of the demise date of RSPF). In a related study, Matyas (2014) indicate that these landfalling tropical cyclones in October are characterized by relatively larger raining areas than the tropical cyclones affecting Florida in other months of the year. Therefore, the implied subsidence and the consequent desiccation after the passage of these large tropical systems over PF would further cause the demise of the RSPF. Alternatively, in the absence of the passage of such tropical systems, the continuing attenuation of the diurnal scales from the summer to the fall seasons over PF (Bastola and Misra 2013) would also result in preconditioning the environment for the demise of the RSPF.

The dramatic onset and demise of the seasonal cycle of the RSPF nearly coincides with a similar cycle of the moisture flux convergence (Fig. 4). Here negative (positive) values denote moisture flux convergence (divergence). Figure 4 shows that the inflection points of the cumulative anomaly curve for daily climatology of rainfall over PF nearly coincides with the corresponding inflection points of the cumulative anomaly curve of the moisture flux convergence. The cumulative anomaly curve of moisture flux convergence in Fig. 4 suggests that prior to the onset of the RSPF there is a prevalence of moisture flux divergence (or weak convergence) that rapidly begins to change to strong convergence after the onset date. Similarly, we observe that at around the time of the demise of the RSPF, the moisture flux convergence becomes weaker than its annual mean climatology. In a modeling sensitivity study of Florida rainy season to variations in Loop Current system, Misra and Mishra (2016) alluded to the changes in the moisture flux

Fig. 4 The time series of daily climatology of rainfall (mm day⁻¹) averaged over PF overlaid with the corresponding cumulative anomaly curve of rainfall and moisture flux convergence (mm day⁻¹). The date of climatological onset (demise) date of the RSPF in Julian day is indicated



convergence from variations to coastal SST affected by the surface currents. Figure 5a shows the composite picture of the moisture flux convergence and moisture flux vectors at the time of the onset of the RSPF, which clearly shows the significant role of the moisture flow from the southwestern edge of the NASH. By the time of the demise of the RSPF (early October) there is moisture flux divergence over PF (Fig. 5b) with NASH gradually receding to the east (Fig.

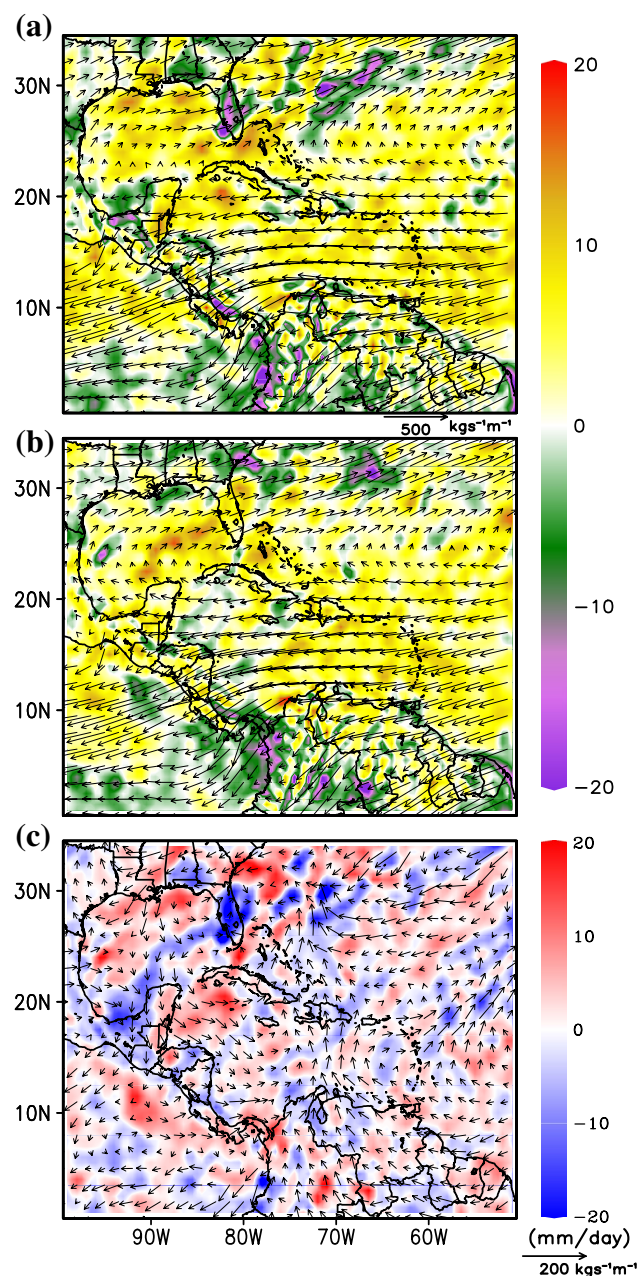


Fig. 5 The composite moisture flux convergence (shaded; mm day^{-1}) and corresponding moisture flux vectors ($\text{kg m}^{-1} \text{s}^{-1}$) from CFSR (Saha et al. 2010) for day of **a** onset and **b** demise of the RSPF, **c** (**a–b**) Negative (positive) shaded values indicate moisture flux convergence (divergence)

S6). It may be noted that terrestrial surface evaporation over Peninsular Florida also follows a similar seasonal cycle as rainfall and moisture flux convergence (not shown), which is also noted in a related observational study of Chan and Misra (2010). This would suggest that local recycling of moisture is an important part of the seasonal cycle of RSPF.

3.3 Seasonal evolution of the upper ocean in the Intra-Americas seas

The evolution of the SST around the onset and the demise of the RSPF is shown in Fig. 6 and S7 respectively. The gradual warming of the IAS prior to the onset of the RSPF is apparent in Fig. 6. This warming of SST is enabled both by corresponding increase in the net atmospheric heat flux into the ocean (Fig. 7) and the oceanic heat transport from the tropical to the subtropical oceans through the seasonal evolution of the Loop Current (see movie SM1). The upper ocean heat transport in SM1 is given by:

$$\vec{H} = \int_{\vec{x}} \int_{z_{26c}}^{z_{\text{surface}}} \vec{V} \theta C_w \rho_w d\vec{x} dz \quad (2)$$

where, C_w and ρ_w are specific heat capacity and density of sea water, \vec{V} and θ are ocean currents and potential temperature, Z_{26c} is the depth of the 26 °C isotherm, which is considered to be an important consideration for sustaining convection in tropical cyclones (Leipper and Volgenau 1972; Shay et al. 2000). Further, it is quite well known that rainfall from landfalling tropical cyclones make significant contribution to RSPF (Knight and Davis 2009; Maxwell et al. 2012, 2013; Prat and Nelson 2013a, b), which draw a significant source of their energy from the warm coastal oceans surrounding PF (Shay et al. 2000; Emanuel 2017). The seasonal cycle of the Yucatan and the Florida Current shows a maximum in summer and a minimum in spring and fall seasons (Johns et al. 2002; Candela et al. 2003; Rousset and Beal 2010), which is consistent with the evolution observed in the movies SM1 and SM2.

In fact, even on the day of onset (day 0), the net heat flux (Fig. 7) is negative (i.e., the flux is directed from the ocean to the atmosphere) for most part of the IAS excluding some parts of the western Gulf of Mexico. However, the build-up of the upper ocean heat content (using the depth of 26 °C isotherm as a proxy) in IAS through day of onset of RSPF is significantly enabled by the maturation of the heat transport enabled by the Loop Current through the Yucatan Peninsula (Fig. SM1). Subsequent to the onset of the RSPF, the atmospheric heat flux (directed from the atmosphere) into the IAS increases appreciably, which further helps in the warming of the upper ocean. Similarly, IAS begins to cool with the retreat of the warmer temperatures from the subtropical latitudes to the deep tropics of the Caribbean

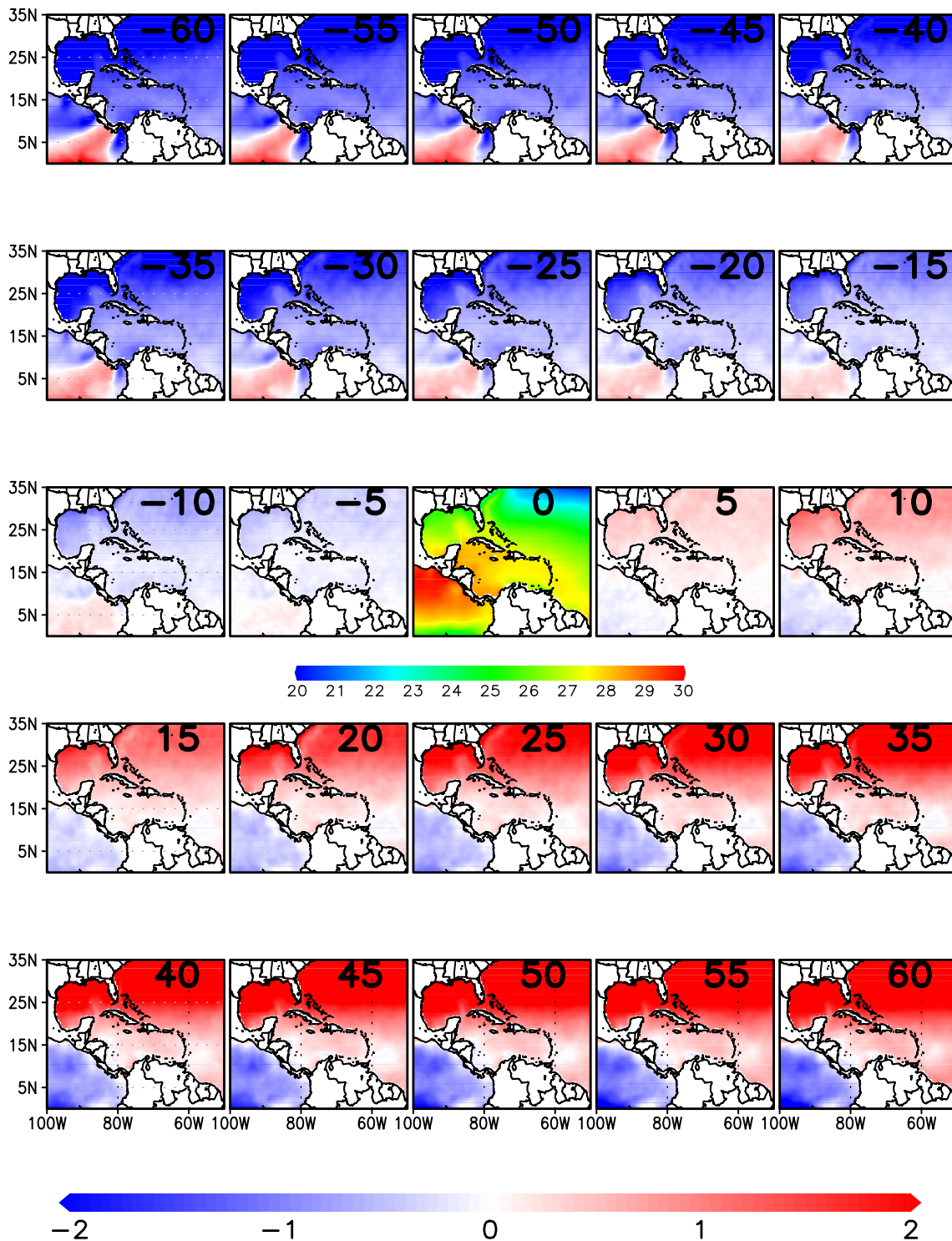


Fig. 6 Seasonal evolution of the daily composite of SST shown as difference from SST on the day of onset of RSPF (°C; day 0) at intervals of 5 days. For the day of onset of RSPF, the full field of SST (°C) is shown

and the tropical Atlantic waters (Fig. S7). This is yet again featured by largely negative atmospheric heat flux by the date of demise (Fig. S8) and rapidly receding oceanic heat transport manifested in the Loop Current (Fig. SM2). It

should also be mentioned that the stronger (weaker) spatial gradients of IAS SST at time of onset (demise) of the RSPF (Figs. 6 and S7) that follows with the seasonal evolution of the Loop Current also has corresponding implications on

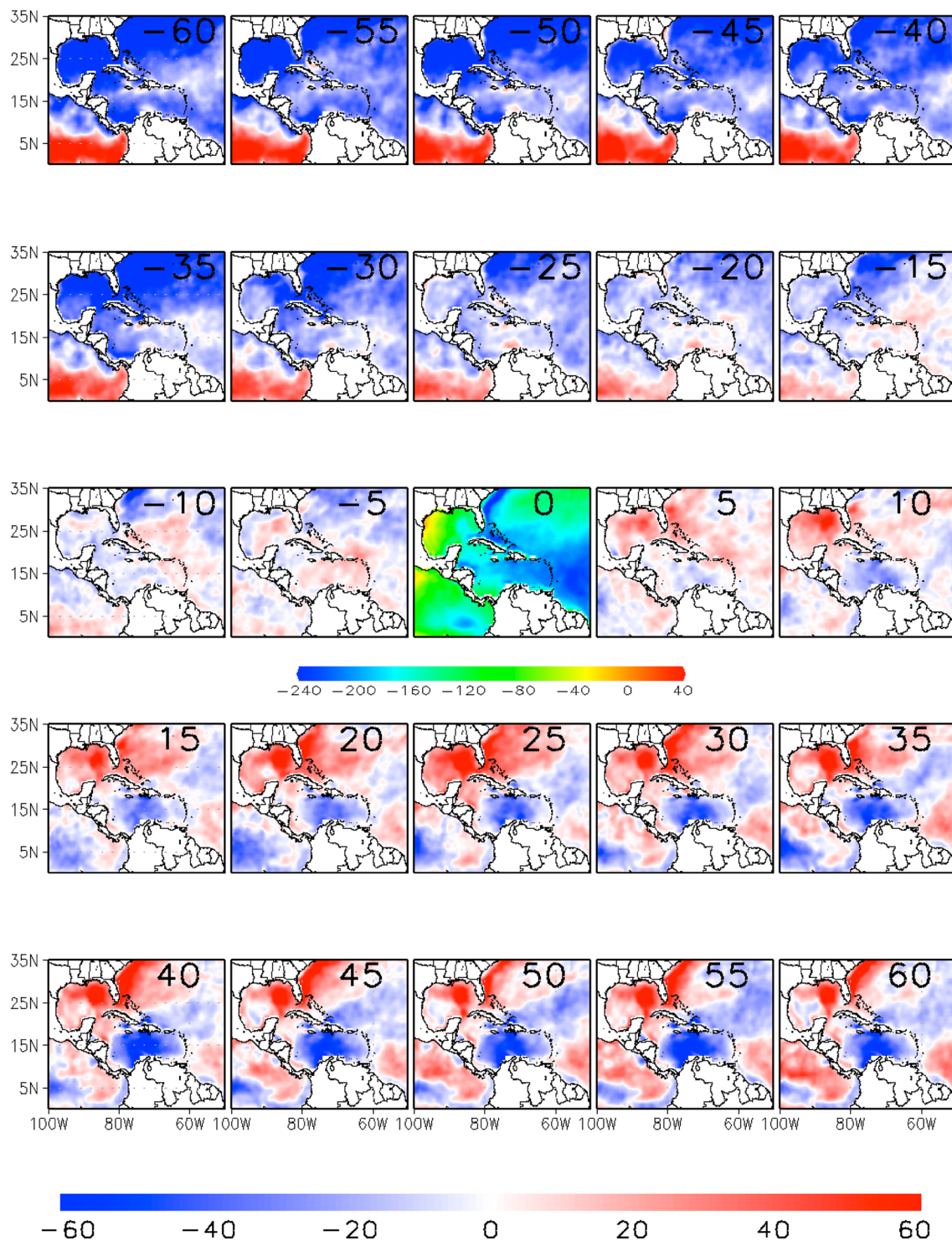


Fig. 7 Seasonal evolution of the daily composite of net atmospheric heat flux shown as difference from the net heat flux on the day of onset of the RSPF (day 0) at intervals of 5 days. The full field of net heat flux (W m^{-2}) is shown for the day of the demise (day 0)

the atmospheric moisture flux convergence over PF through its influence on surface evaporation from the coastal oceans, low level atmospheric moisture and surface winds.

3.4 Interannual variability

As noted in Fig. S2 and in Table 1, there is considerable year-to-year variation in the onset and demise dates, and

Table 1 The mean, standard deviation and correlations between onset date, demise date, season length, and total seasonal rainfall anomalies of the RSPF

	Onset date	Demise date	Season length	Seasonal rainfall anomalies
Mean	148 (Julian day)	277 (Julian day)	129 (days)	826 (mm)
Standard deviation	15 (days)	16 (days)	22 (days)	152 (mm)
Correlations				
Onset date	1	0.05	-0.67	-0.42
Demise date	0.05	1	0.71	0.56
Season length	-0.67	0.71	1	0.71

Values significant at the 95% confidence interval by bootstrap method (Wilkes 2011) are in bold

consequently in the seasonal length of the RSPF. In Florida, tourism and agriculture are the first and the second largest industries, that do critically depend on the seasonal climate and its variations. Therefore, efforts to understand the variations and the predictability of the RSPF would potentially benefit both of these industries at the outset. The growing renewable solar and wind energy industries of Florida are also likely to benefit from the predictability studies of the RSPF.

From Table 1 it is clear that the onset date has a significant influence on the seasonal length and consequently the accumulated seasonal rainfall anomalies of the RSPF. A -0.67 and -0.42 correlation in Table 1 with onset date variations of RSPF suggests that early (late) onset is associated with longer (shorter) seasonal length and anomalously wet (dry) RSPF respectively. This is a very useful teleconnection as it is possible to use the observed monitoring of the variations of the onset date to anticipate the likelihood of the seasonal rainfall anomalies of the subsequent RSPF. Similarly, the demise date also shows significant correlation of its anomalies with the seasonal length and rainfall anomalies of the preceding RSPF season.

The correlation of the onset and demise dates of the RSPF with corresponding seasonal rainfall anomalies over PF is shown in Fig. 8a, b respectively. As noted in Table 1, the onset date of the RSPF has a widespread influence on the subsequent seasonal rainfall anomalies across PF (Fig. 8a), with early (late) onset associated with widespread increase (decrease) of the seasonal rainfall anomalies. Likewise, excess (deficit) seasonal rainfall anomalies over PF is associated with the late (early) demise date variations of the RSPF (Fig. 8b). The external forcing for variations of the onset and demise date of the RSPF have to be thoroughly investigated in future studies. However, Misra and DiNapoli (2013) indicate to variations of ENSO and the AWP to describe the interannual variability of the onset and demise of the wet season of PF respectively. Figure S2, also shows longer-term (intra and inter-decadal) variations that could easily be influenced by the variations in the Loop Current (Misra and Mishra 2016), the upper limb of the Atlantic Meridional

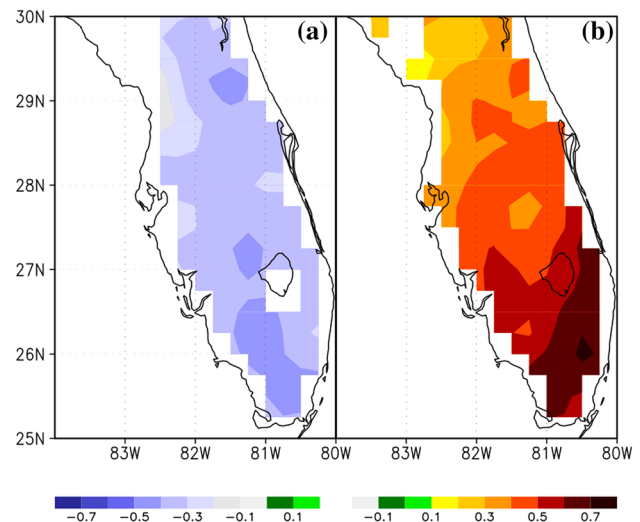


Fig. 8 The correlation of seasonal mean rainfall anomaly with corresponding **a** onset date and **b** demise date of the RSPF. Only significant values at 95% confidence interval according to bootstrap (Wilkes 2011) is shown

Overturning Circulation (AMOC). In fact, Enfield et al. (2001) allude to the influence of the Atlantic multidecadal oscillation on rainfall over south-central Florida. More recently, in a modeling study of Misra and Mishra (2016), it is shown that the length and the distribution of the daily rainfall of the RSPF is influenced by the variations in the Florida Currents.

4 Conclusions

The seasonality of the Rainy Season of Peninsular Florida (RSPF) is examined in this study. The spectacular arrival of rains in Peninsular Florida (PF) from around 4 mm day^{-1} prior to onset to around 12 mm day^{-1} on the day of the onset of the rainy season is a robust phenomenon of the RSPF. Similarly, demise of the RSPF is equally dramatic with rain rates over 12 mm day^{-1} a day prior to demise receding to

below 5 mm day⁻¹ on the day of the demise of the rainy season. This literal flipping on and off of the RSPF season involves a co-evolution of other associated atmospheric and upper ocean variables. The realization of such strong seasonal cycle of rainfall is associated with similar robust seasonal changes in the low level atmospheric winds, SST in the IAS, which consequently builds the terrestrial moisture flux convergence over PF. The seasonal cycle of the net atmospheric heat flux, upper ocean circulation associated with the Loop Current system, builds the upper ocean heat content in the neighboring oceans of PF, which fosters the prolonged sustenance of the RSPF. Our composites isolate the potential role of the cold frontal passages providing the trigger for the dramatic onset of the RSPF. Similarly, we find that in a large fraction of the years the desiccation of the atmospheric column after the passage of tropical cyclones over PF in addition to the continuing attenuation of the diurnal scales from the summer to the fall season leads to the demise of the RSPF.

The interannual variations of the onset and demise days, seasonal length, and wet seasonal rainfall anomalies of the RSPF is significant. We have not dwelled extensively into the causes of their variability, although some previous studies have attributed variations associated with ENSO and AWP variations as some of the significant factors affecting the interannual variations of RSPF. Furthermore, some of these metrics of RSPF also suggest longer-term variations, which is not surprising given that they share the seasonal evolution with the Loop Current, which is part of the upper limb of the Atlantic Meridional Overturning Circulation (AMOC). It is however noteworthy that the seasonal rainfall anomalies of the RSPF are strongly associated with the variations of its onset and demise date. This does raise the hope of predicting the likelihood of the following wet season anomalies of the RSPF by just monitoring its onset date while also attempting to use seasonal prediction models to further advance the lead time of such predictions. The post-script of the RSPF season can also be analyzed in the context of the variations of the demise date.

This recognition of the co-evolution of the seasonal cycle of several of the atmospheric and upper ocean variables with the RSPF provides an important marker to understand its variations across a spectrum of temporal scales. For example, for any significant changes to have occurred in RSPF either in the past (paleoclimate) or projected to occur in the future will likely have to be associated with large-scale changes in the IAS including changes to ocean currents, heat content and changes to NASH.

Acknowledgements The authors gratefully acknowledge the financial support given by NOAA (NA12OAR4310078), the Earth System Science Organization, Ministry of Earth Sciences, Government of India (Grant Number MM/SERP/FSU/2014/SSC-02/002) to conduct this

research under Monsoon Mission and the South Florida Water Management District (PO 039231).

References

- Bastola S, Misra V, Li H (2013) Seasonal hydrological forecasts for watersheds over the Southeastern United States for the boreal summer and fall seasons. *Earth Interact* 17(25):1–22. <https://doi.org/10.1175/2013EI000519.1>
- Brezonik PL, Hendry CD, Edgerton ES, Schulze RL, Crisman TL (1983) Acidity, nutrients and minerals in atmospheric precipitation over Florida: deposition patterns, mechanisms, and ecological effects. EPA-600/3-83-004. US Environmental Protection Agency, Corvallis
- Candela J, Tanahara S, Crepon M, Barnier B, Sheinbaum J (2003) Yucatan channel flow: observations versus CLIPPER ATL6 and MERCATOR PAM models. *J Geophys Res* 108(C12):3385–3408. <https://doi.org/10.1029/2003jc001961>
- Carr MH, Zwick PD (2016) Water 2070: mapping Florida's future-alternative patterns of water use in 2070. Technical Report of the Geoplan Center, University of Florida. <http://1000friendsofflorida.org/water2070/wp-content/uploads/2016/11/water2070technical-reportfinal-text-TOC.pdf>
- Chan SC, Misra V (2010) A diagnosis of the 1979–2005 extreme rainfall events in the southeastern United States with isentropic moisture tracing. *Mon Weather Rev* 138(4):1172–1185
- Chen M, Shi W, Xie P, Silva V, Kousky VE, Wayne Higgins R, Janowiak JE (2008) Assessing objective techniques for gauge-based analyses of global daily precipitation. *J Geophys Res Atmos* 113(D4)
- Davis H (1996) Hydrogeologic investigation and simulation of groundwater flow in the Upper Floridan aquifer of north-central Florida and southwestern Georgia and delineation of contributing areas for selected City of Tallahassee, Florida, water-supply wells. US Geological Survey; Earth Science Information Center, Open-File Reports Section (distributor), pp 95–4296
- Emanuel K (2017) Will global warming make hurricane forecasting more difficult? *Bull Am Soc* 98:495–501
- Enfield DB, Mestas-Nuñez AM, Trimble PJ (2001) The Atlantic multi-decadal oscillation and its relation to rainfall and river flows in the continental US. *Geophys Res Lett* 28(10):2077–2080
- Johns WE, Townsend TL, Fratantoni DM, Wilson WD (2002) On the Atlantic inflow to the Caribbean Sea. *Deep Sea Res Part I* 49(2):211–243
- Knight DB, Davis RE (2009) Contribution of tropical cyclones to extreme rainfall events in the southeastern United States. *J Geophys Res Atmos* 114(D23)
- Leipper DF, Volgenau D (1972) Hurricane heat potential of the Gulf of Mexico. *J Phys Oceanogr* 2(3):218–224
- Li W, Li L, Fu R, Deng Y, Wang H (2011) Changes to the North Atlantic subtropical high and its role in the intensification of summer rainfall variability in the southeastern United States. *J Clim* 24:1499–1506
- Matyas CJ (2014) Conditions associated with large rain-field areas for tropical cyclones landfalling over Florida. *Phys Geogr* 35:93–106
- Maxwell JT, Soulé PT, Ortegren JT, Knapp PA (2012) Drought-busting tropical cyclones in the southeastern Atlantic United States: 1950–2008. *Ann Assoc Am Geogr* 102(2):259–275
- Maxwell JT, Ortegren JT, Knapp PA, Soulé PT (2013) Tropical cyclones and drought amelioration in the Gulf and southeastern coastal United States. *J Clim* 26(21):8440–8452
- Misra V, DiNapoli SM (2013) Understanding the wet season variations over Florida. *Clim Dyn* 40(5–6):1361–1372

- Misra V, Mishra A (2016) The oceanic influence on the rainy season of Peninsular Florida. *J Geophys Res Atmos* 121(13):7691–7709
- Nag B, Misra V, Bastola S (2015) Validating ENSO teleconnections on southeastern United States winter hydrology. *Earth Interact.* <https://doi.org/10.1175/EI-D-14-0007.1>
- Noska R, Misra V (2016) Characterizing the onset and demise of the Indian summer monsoon. *Geophys Res Lett* 43(9):4547–4554
- Obeysekera J, Browder J, Hornung L, Harwell MA (1999) The natural South Florida system I: climate, geology, and hydrology. *Urban Ecosyst* 3:223–244
- Prat OP, Nelson BR (2013a) Precipitation contribution of tropical cyclones in the southeastern United States from 1998 to 2009 using TRMM satellite data. *J Clim* 26(3):1047–1062
- Prat OP, Nelson BR (2013b) Mapping the world's tropical cyclone rainfall contribution over land using the TRMM multi-satellite precipitation analysis. *Water Resour Res* 49(11):7236–7254
- Price RM, Swart PK (2006) Geochemical indicators of groundwater recharge in the surficial aquifer system, Everglades National Park, Florida, USA. *Geol Soc Am Spec Pap* 404:251–266
- Ropelewski CF, Halpert MS (1987) Global and regional scale precipitation patterns associated with the El Niño/Southern Oscillation. *Mon Weather Rev* 115:1606–1626
- Rousset C, Beal LM (2010) Observations of the Florida and Yucatan currents from a Caribbean cruise ship. *J Phys Oceanogr* 40(7):1575–1581
- Saha S, Moorthi S, Pan HL, Wu X, Wang J, Nadiga S, Tripp P, Kistler R, Woollen J, Behringer D, Liu H (2010) The NCEP climate forecast system reanalysis. *Bull Am Meteorol Soc* 91(8):1015–1057
- Schmidt N, Lipp EK, Rose JB, Luther ME (2001) ENSO influences on seasonal rainfall and river discharge in Florida. *J Clim* 14:615–628
- Shay LK, Goni GJ, Black PG (2000) Effects of a warm oceanic feature on Hurricane Opal. *Mon Weather Rev* 128(5):1366–1383
- Sneyers R, Vandiepenbeeck M, Vanilieder R, Demarée GR (1990) Climatic changes in Belgium as appearing from the homogenized series of observations made in Brussels–Uccle (1933–1988). In: Schietecat GD (ed) *Contributions à l'étude des changements de climat*, vol 124. Institut Royal Meteorologique de Belgique, Publications Série, Bruxelles, pp 17–20
- Stefanova L, Misra V, O'Brien JJ, Chassignet EP, Hameed S (2012) Hindicast skill and predictability of APCC models for precipitation and surface temperature anomalies over the Southeast United States. *Clim Dyn* 38:161–173
- Webb SD (1990) Historical biogeography. In: Myers RL, Ewel JJ (eds) *Ecosystems of Florida*. University of Central Florida Press, Orlando, pp 70–100
- Wilkes D (2011) *Statistical methods in the atmospheric sciences*, 2nd edn. Academic Press, Oxford, p 704
- Xie P, Yatagai A, Chen M, Hayasaka T, Fukushima Y, Liu C, Yang S (2007) A gauge based analysis of daily precipitation over East Asia. *J Hydrometeorol* 8:607–626